Electronic Supplementary Material (ESI) for Soft Matter.
This journal is © The Royal Society of Chemistry 2021

Electronic Supplementary Information

Soft Synthetic Microgels as Mimics of Mycoplasma

Dominic Büning[1], Jens Schumacher[1], Alexander Helling[2], Ramzi Chakroun[3], Franka Ennen-Roth[1], Andre Harald Gröschel[3], Volkmar Thom[2], Mathias Ulbricht[1,*]

[1] Lehrstuhl für Technische Chemie II, Universität Duisburg-Essen, 45117 Essen, Germany

[2] Sartorius Stedim Biotech GmbH, August-Spindler-Straße 11, 37079 Göttingen, Germany

[3] Institute of Physical Chemistry, University of Münster, Corrensstr. 28-30, 48149 Münster, Germany

Table of Contents

ESI-1: Setup for cake compressibility measurements

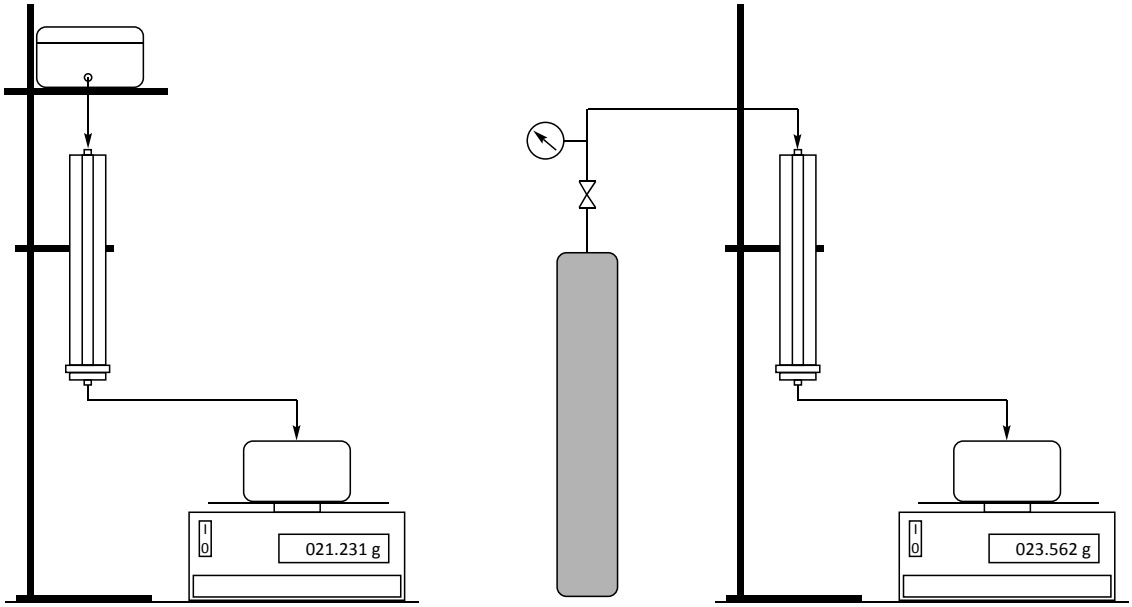

Fig. SI-1: Schematic depiction of the filtration setup used in cake filtration measurement; setup using hydrostatic pressure (ΔP < 100 mbar; left) and artificial gas pressure (ΔP ≥ 100 mbar; right).

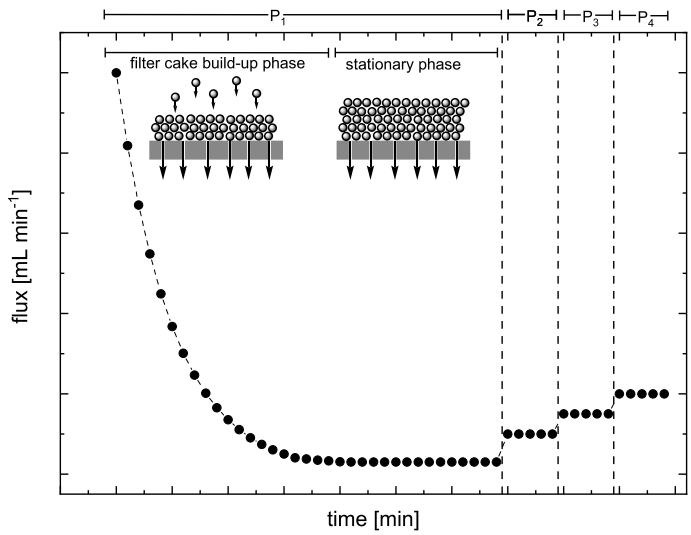

Fig. SI-2: Schematic depiction of the cake filtration experiment for the characterization of the particle deformability; after the filter cake buildup the sequential increase of the transmembrane pressure ($P_1 < P_2 < P_3 < P_4$) was done after a constant flux was reached.

ESI-2: Full recipes of microgel synthesis by inverse miniemulsion polymerization

Tab. SI-1. Recipes of poly(acrylamide) microgel synthesis by inverse miniemulsion polymerization.

Crosslinker content [a]	(w/w) [%]	4.76
Polymeric solid content [b]	(w/w) [%]	20.8
<u>dispersed</u>		
AAm	[mg]	800
MBAAm	[mg]	40
NaCl	[mg]	94
H_2O	[g]	3.2
<u>continuous</u>		
Span80	[g]	1.2
Cyclohexan	[g]	50
AIBN	[mg]	128

[a] In relation to the total polymeric solid content; [b] total polymeric solid content, assuming 100% conversion and incorporation of all monomers into the microgels polymeric network, relative to the used water mass.

Tab. SI-2. Recipes of poly(acrylamide-co-sodium acrylate) microgel synthesis by inverse miniemulsion polymerization (I); under varied crosslinker content, constant polymeric solid content (≈ 21% (w/w)) and constant content of sodium (9.52% (w/w)).

Crosslinker content [a]	(w/w) [%]	0.50	2.44	4.76 *	6.98	9.09	20.0
Polymeric solid content [b]	(w/w) [%]	20.1	20.4	20.8	21.2	21.6	23.8
<u>dispersed</u>							
AAm	[mg]	720	720	720	720	720	720
MBAAm	[mg]	4	20	40	60	80	200
AANa	[mg]	80	80	80	80	80	80
NaCl	[mg]	94	94	94	94	94	94
H_2O	[g]	3.2	3.2	3.2	3.2	3.2	3.2
<u>continuous</u>							
Span80	[g]	1.2	1.2	1.2	1.2	1.2	1.2
Cyclohexane	[g]	50	50	50	50	50	50
AIBN	[mg]	128	128	128	128	128	128

[a] In relation to the total polymeric solid content; [b] total polymeric solid content, assuming 100% conversion and incorporation of all monomers into the microgels polymeric network, relative to the used water mass; * has been referred to as super soft microgel.

Tab. SI-3. Recipes of poly(acrylamide-co-sodium acrylate) microgel synthesis by inverse miniemulsion polymerization (II); under varied polymeric solid content, constant crosslinker content (4.76 % (w/w)) and constant content of sodium (9.52% (w/w)).

Polymeric solid content [a]	(w/w) [%]	2.56	10.1	20.8 *	30.0	40.1	50.0 **
Crosslinker content [b]	(w/w) [%]	4.76	4.71	4.76	4.73	4.71	4.74
<u>dispersed</u>							
AAm	[mg]	72	310	720	1180	1840	2750
MBAAm	[mg]	4	17	40	65	101	152
AANa	[mg]	8	34	80	128	202	303
NaCl	[mg]	94	94	94	94	94	94
H_2O	[g]	3.2	3.2	3.2	3.2	3.2	3.2
<u>continuous</u>							
Span80	[g]	1.2	1.2	1.2	1.2	1.2	1.2
Cyclohexane	[g]	50	50	50	50	50	50
AIBN	[mg]	128	128	128	128	128	128

[a] total polymeric solid content, assuming 100% conversion and incorporation of all monomers into the microgels polymeric network, relative to the used water mass; [b] In relation to the total polymeric solid content; * has been referred to as super soft and ** as soft microgel.

Tab. SI-4. Recipes of poly(acrylamide-co-sodium acrylate) microgel synthesis by inverse miniemulsion polymerization (III); under varied content of sodium acrylate, constant crosslinker content (4.76 % (w/w)) and constant polymeric solid content (≈ 21% (w/w)).

Sodium acrylate content [a]	(w/w) [%]	0	4.76	9.52*	14.3
Crosslinker content [a]	(w/w) [%]	4.76	4.76	4.76	4.76
Polymeric solid content [b]	(w/w) [%]	20.8	20.8	20.8	20.8
<u>Dispers</u>					
AAm	[mg]	800	760	720	680
MBAAm	[mg]	40	40	40	40
AANa	[mg]	0	40	80	120
NaCl	[mg]	94	94	94	94
H_2O	[g]	3.2	3.2	3.2	3.2
<u>continuous</u>					
Span80	[g]	1.2	1.2	1.2	1.2
Cyclohexan	[g]	50	50	50	50
AIBN	[mg]	128	128	128	128

[a] In relation to the total polymeric solid content; [b] total polymeric solid content, assuming 100% conversion and incorporation of all monomers into the microgels polymeric network, relative to the used water mass; ***** has been referred to as super soft microgel.

ESI-3: ATR FT-IR spectra for poly(AAm-co-AANa) microgels

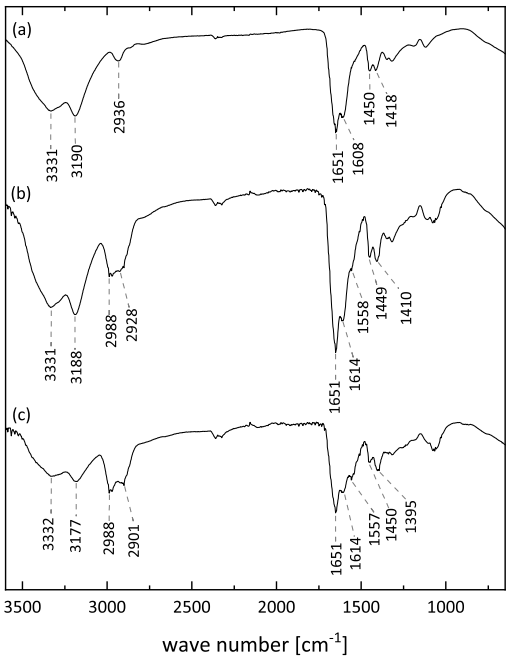

Fig. SI-3: IR spectra for poly(acrylamide-co-sodium acrylate) microgel, consisting of 0% (w/w) (a), 10% (w/w) (b) or 15% (w/w) (c) sodium acrylate segments.

ESI-4: Elemental analysis data for poly(AAm-*co*-AANa) microgels

The analysis of the microgel composition was carried out by means of elemental analysis of the carbon, hydrogen, nitrogen and oxygen content of the freeze-dried samples. For the interpretation of the gathered data, the theoretical contents of this elements were calculated for each sample, assuming a quantitative incorporation of all polymerizable monomers in the polymeric network. Additionally, the contribution of the initiator (*i.e.* AIBN) to the polymer composition was taken into account. For ideal inverse miniemulsion polymerization, the droplet nucleation mechanism can be expected to be the dominant pathway. [1] Radicals, exclusively formed in the continuous phase (*i.e.* cyclohexane phase) by decomposition of the hydrophobic initiator, are supposed to primarily enter the water droplets as hydrophilic oligoradicals to initiate the polymerization and thus being incorporated in the forming hydrogel network. [1] Do to this mechanism, the accurate estimation of the amount of incorporated initiator components (*i.e.* 2-cyanoprop-2-yl radicals) is not feasible. Therefore, two unrealistic hypothetic cases have been considered here, similar to the approach presented already in our previous study. [2] In the first case it was assumed that no 2-cyanoprop-2-yl radical was incorporated in the network (Theo.I), while in the second case it was assumed that every theoretically producible radical was incorporated (Theo.II). A realistic estimation of the theoretical element contents and ratios was achieved by considering values between both extreme cases (*cf.* Fig. SI-4).

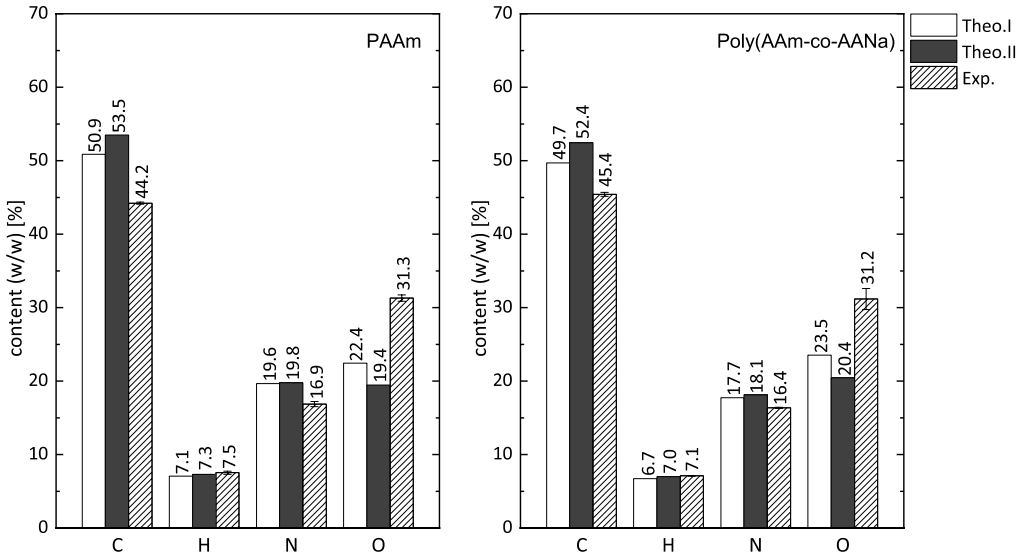

Fig. SI-4: C, H, N and O content of polyacrylamide (left) and poly(acrylamide-*co*-sodium acrylate) (right) microgels related to the dry polymeric mass; 10% (w/w) theoretical sodium acrylate segments (right); theoretical element values have been calculated assuming 0% (Theo.I) or 100% (Theo.II) of initiator radicals incorporated in the microgels; experimental values (Exp.).

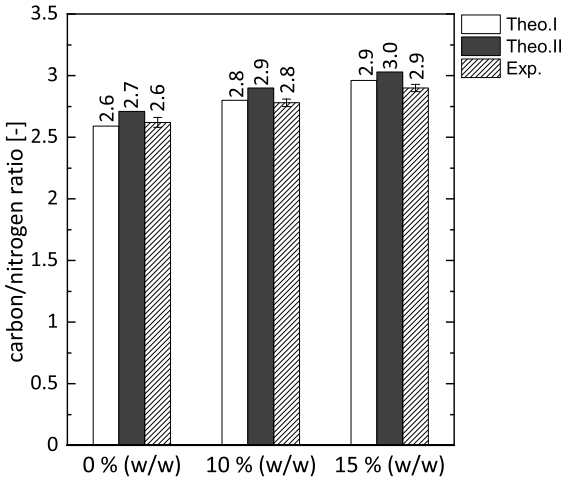

Fig. SI-5: Carbon-to-nitrogen ratio of poly(acrylamide-co-sodium acrylate) microgels containing 0%, 10% or 15% (w/w) theoretical sodium acrylate segments; theoretical element values have been calculated assuming 0% (Theo.I) or 100% (Theo.II) of initiator radicals incorporated in the microgels; experimental values (Exp.).

ESI-5: Additional DLS data on miniemulsions with varied crosslinker content

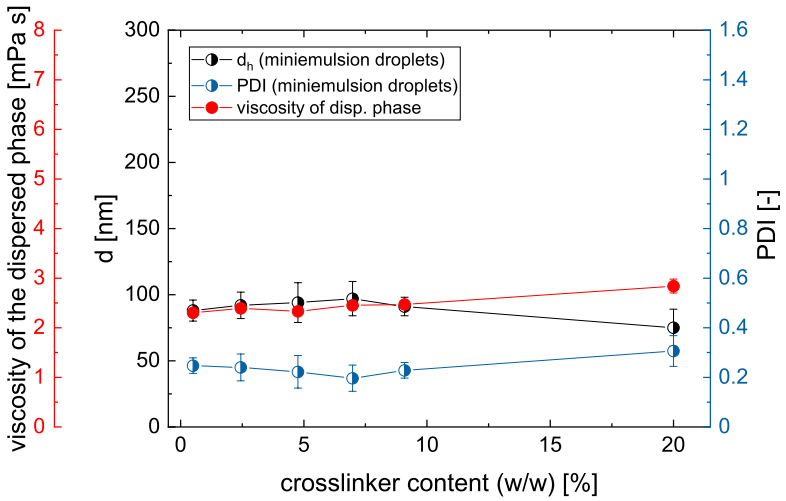

Fig. SI-6: Comparison of the mean droplet size in cyclohexane and the viscosity of the dispersed phase on the crosslinker content at constant polymeric solid content (20 – 22% (w/w)) and content of sodium acrylate (9.52% (w/w)).

ESI-6: Theoretical estimation of the dispersed phase volume expansion

Prior to an estimation of osmotic concentration in the aqueous inverse miniemulsion droplets, (ESI-7) or theoretical droplet number (ESI-10), a precise knowledge of the dispersed phase volume is required. Consequently, there is a need to estimate the volume expansion, induced by the solubilization of different synthesis components, *e.g.* monomers and osmotic agent, in water. This has been done by using both theoretical *ab initio* calculations of the partial volumes of the individual components according to Durchschlag et al. [3] and experimental assessment of the resulting volume. Figure SI-7 reveals a significant volume expansion effect, which turned out to be minor with increasing crosslinker content, but significant with increase in polymeric solid content. The real volume of the dispersed phase increased from 3.3 mL (2.56% (w/w) polymeric solid content) towards 6.0 mL (50% (w/w) polymeric solid content). Contrary to that, an increase of the crosslinker content resulted in caused a volume expansion from 3.8 mL to 3.9 mL, which, in fact, can also be related to a slightly increase in polymeric solid content, *i.e.* from 20.1% to 23.8% (w/w).

It has been observed that for high polymeric solid contents, *i.e.* 40% to 50% (w/w), there is a significant difference between the theoretical estimation and the experimental data. This, could indicate that the spread between theoretical and the apparent volume, the so-called excess volume, has not been adequately described for all compositions by the used *ab initio* method. In particular, polyelectrolyte and other ionic components are able to cause a large increase in their apparent molar volume with their concentration. [4] Therefore, experimentally assessed volumes has been used in the following calculations (cf. ESI-7, ESI-10) exclusively.

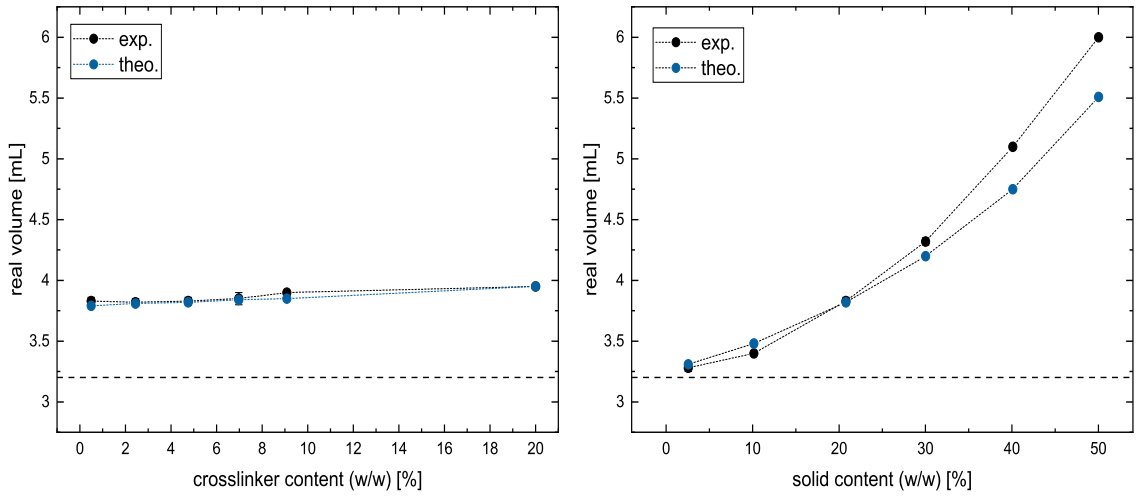

Fig. SI-7: Real volume of the dispersed phase, taking into account the volume expansion effect, induced by solubilization of monomers and the osmotic agent; variation of the crosslinker content (left); variation of the polymeric solid content (right); experimental data has been gathered by volumetry; theoretical data has been assessed by ab initio calculation of the partial volumes, according to Durchschlag et al. [3]

ESI-7: Osmotic concentrations of the dispersed phase and its impact on droplet size

In order to estimate the impact of the used sodium acrylate, its content and the total polymeric solid content, on the osmotic concentration $c_{osm.}$ of the aqueous dispersed phase, the later was calculated by the following relation SI-1. [5, 6] This expression is taking into account the ideal gas constant R and the absolute temperature T. It must be noted this approximation is valid for very low concentrated only.

$$\lim_{c \to 0} \Pi_{osm.} = R\,T\,c_{osm.} \qquad \text{(SI-1)}$$

In addition, the osmotic concentration has been calculated by an approximation of Morse et al. (*cf.* equation SI-2), taking into account the osmolality $b_{osm.}$ instead of $c_{osm.}$, which can be considered as valid, also in higher concentrations. [7]

$$\Pi_{osm.} = R\,T\,b_{osm.} \qquad \text{(SI-2)}$$

The Laplace pressure in a miniemulsion droplet can be calculated from the mean droplet radius r and the interfacial tension γ_{LL} at the liquid-liquid interface, between the disperse and the continuous phase.

$$P_{Laplace} = \frac{2\,\gamma_{LL}}{r} \qquad \text{(SI-3)}$$

As inverse miniemulsions tend to form a dynamic equilibrium state between $\Pi_{osm.}$ and $P_{Laplace}$, [8] Willert provided the hypothesis that there is a reciprocal relationship between r and $c_{osm.}$(cf. equation SI-4). [9]

$$P_{Laplace} = \Pi_{osm.} \rightarrow R\,T\,c_{osm.} = \frac{2\,\gamma_{LL}}{r} \qquad \text{(SI-4)}$$

Tab. SI-5. Osmotic concentration of acrylamide containing miniemulsions, with and without sodium acrylate and the theoretic impact on the mean radius of the droplets, according to Willert. [9]

	Concentration of osmotic agents				mean droplet radius		
	c (NaCl)	c (AANa)	$c_{osm.}$ §	$b_{osm.}$	theo. I †	theo. II ‡	exp.
	[mM]	[mM]	[mM]	[mol kg^{-1}]	[nm]	[nm]	[nm]
AAm	500	0	412	0.50	-	-	85 ± 8
AAm/AANa	500	266	642	0.77	54 ± 5	55 ± 5	46 ± 5

§ The osmotic concentration has been calculated taking into account the real volumes of the dispersed phase (ESI-6); † Calculation of the osmotic pressure based on equation SI-1; [5, 6] ‡ Calculation of the osmotic pressure based on equation SI-2, according to MORSE et al.. [7, 10]

Tab. SI-6. Impact of the polymeric solid content on the osmotic concentration and mean droplet size.

Polymeric solid content	Concentration of osmotic agents				mean droplet radius		
	c (NaCl)	c (AANa)	$c_{osm.}$ §	$b_{osm.}$	theo. I †	theo. II ‡	exp.*
[% (w/w]	[mM]	[mM]	[mM]	[mol kg^{-1}]	[nm]	[nm]	[nm]
2,56	500	27	516	0,59	-	-	52 ± 3
10,15	500	113	601	0,86	45 ± 3	35 ± 2	40 ± 4

§ The osmotic concentration has been calculated taking into account the real volumes of the dispersed phase (ESI-6); † Calculation of the osmotic pressure based on equation SI-1; [5, 6] ‡ Calculation of the osmotic pressure based on equation SI-2, according to MORSE et al. [7, 10]

Tab. SI-7. Impact of content of sodium acrylate on the osmotic concentration and mean droplet size.

Content of sodium acrylate	Concentration of osmotic agents				mean droplet radius		
	c (NaCl)	c (AANa)	$c_{osm.}$ §	$b_{osm.}$	theo. I †	theo. II ‡	exp.*
[% (w/w]	[mM]	[mM]	[mM]	[mol kg^{-1}]	[nm]	[nm]	[nm]
0	500	0	412	0,50	-	-	85 ± 9
4,76	500	133	531	0,64	66 ± 7	67 ± 7	72 ± 4
9,52	500	266	642	0,77	54 ± 5	55 ± 6	46 ± 6
14,29	500	399	753	0,90	46 ± 5	47 ± 5	95 ± 3

§ The osmotic concentration has been calculated taking into account the real volumes of the dispersed phase (ESI-6); † Calculation of the osmotic pressure based on equation SI-1; [5, 6] ‡ Calculation of the osmotic pressure based on equation SI-2, according to MORSE et al. [7, 10]

ESI-8: Additional data on microgels electrokinetic properties

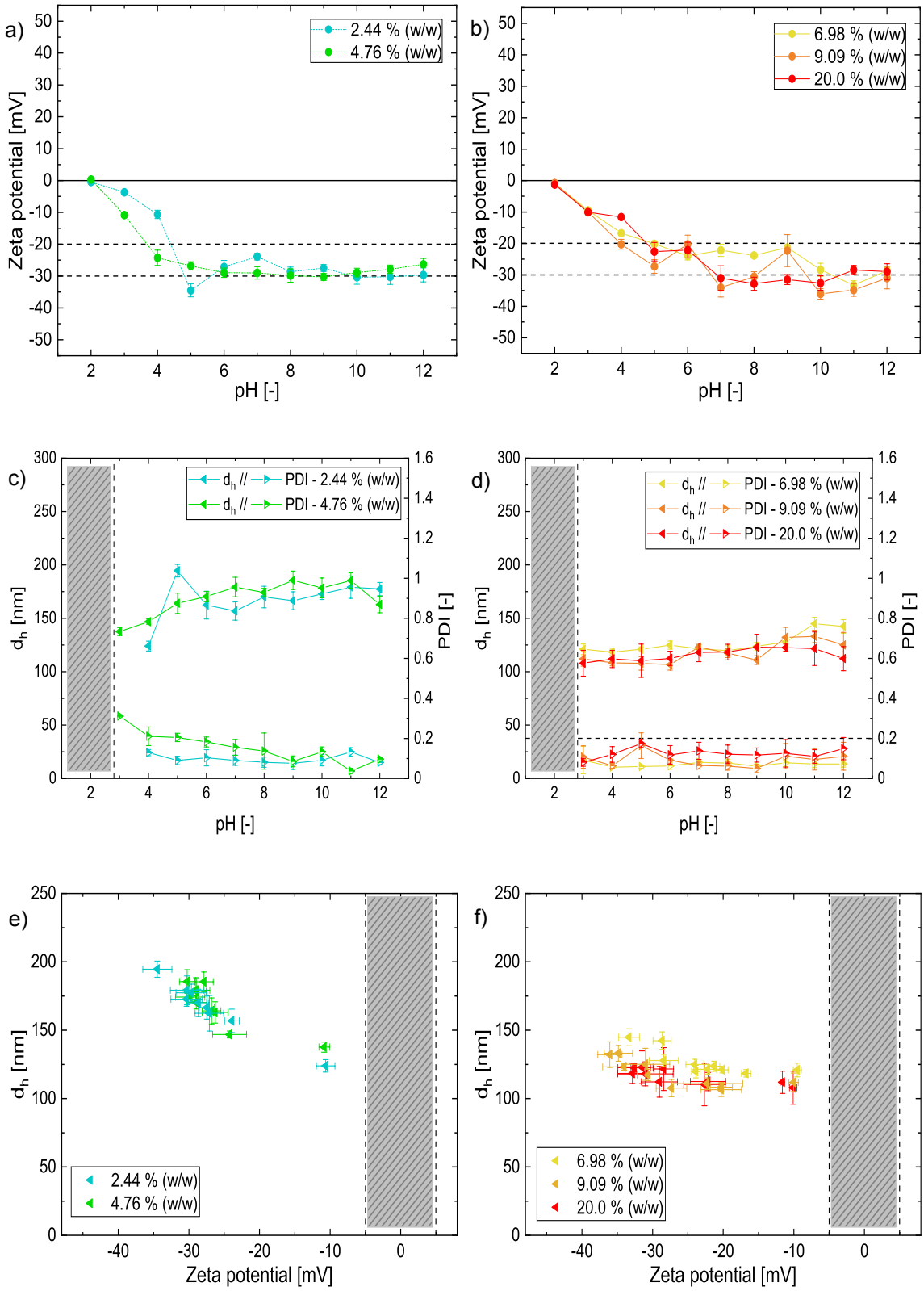

Fig. SI-8: Electrokinetic properties of poly(acrylamide-co-sodium acrylate) microgels in water under varied crosslinker content, constant polymeric solid content (20 – 22 % (w/w)) and content of sodium acrylate (9.52 % (w/w)); (a-b) apparent zeta potential and (c-d) hydrodynamic mean diameter in relation

to pH; (e-f) hydrodynamic mean diameter in relation to the apparent zeta potential, area of instability is marked as grey band.

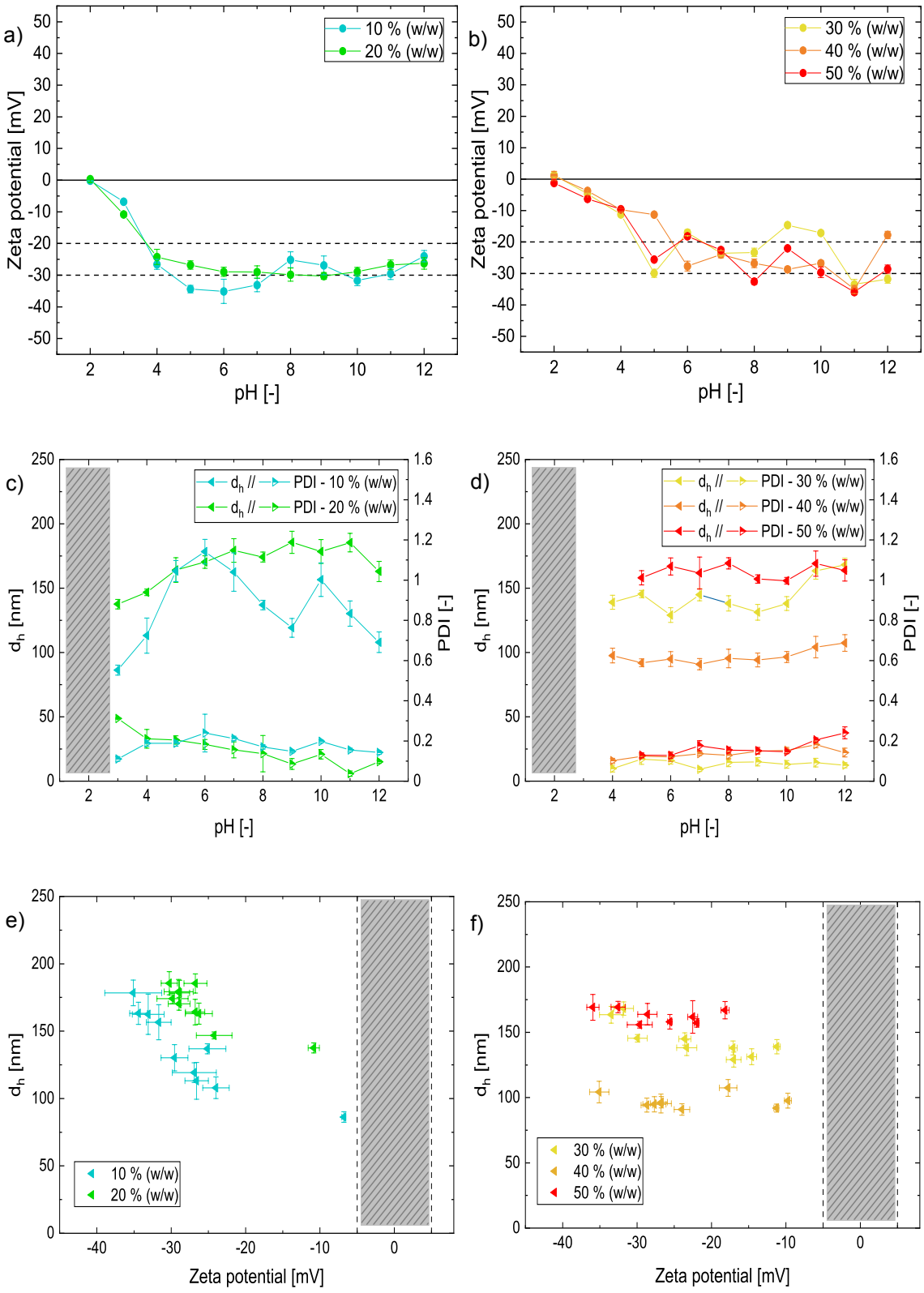

Fig. SI-9: Electrokinetic properties of poly(acrylamide-co-sodium acrylate) microgels in water under varied polymeric solid content, constant crosslinker content (4.76 % (w/w)) and content of sodium acrylate (9.52 % (w/w)); (a-b) apparent zeta potential and (c-d) hydrodynamic mean diameter in relation

to pH; (e-f) hydrodynamic mean diameter in relation to the apparent zeta-potential, area of instability is marked as grey band.

ESI-9: Considerations for the theoretical calculations of the microgels molar mass

The microgels molar mass or the mass per microgel particle can be considered as important parameter for the calculation of microgel number-based concentrations and challenges per filtrated area, particular relevant for perspective filtration studies. Besides an experimental investigation by means of static light scattering (*cf.* ESI-10), this parameter can be roughly estimated from the number of the initially generated miniemulsion droplets, as this reaction cavities acting as precursors for the later microgels, due to the nanoreactor concept of the inverse miniemulsion polymerization. [11]

In a first step, the average volume per droplet has been calculated from the average droplet diameter, which has been measured as number weighted average by means of dynamic light scattering. Under the assumption that the calculated average droplet volume is a sufficiently accurate description of all droplets, *i.e.* assuming a rather monodisperse particle distribution, this and the total volume of the disperse phase can be used to estimate a number of particles per batch in a second step. Finally, under the assumption that all polymerizable components are statistically equally to each droplet, nanoreactor concept, and have been fully integrated in the polymeric network, a theoretic molar mass can be estimated. A summary of all relevant parameters can be found in the following Tab. SI-8 and Tab. SI-9.

Tab. SI-8. Relevant parameter for the theoretical estimation of the microgels molar mass (I); varied crosslinker content and constant polymeric solid content (≈ 21 % (w/w)); *real volume of the disperse phase according to ESI-6; ** hydrodynamic man diameter measured as number weighted average by means of dynamic light scattering

Crosslinker content	(w/w) [%]	0.50	2.44	4.76	6.98	9.09	20.00
Polymeric solid content	(w/w) [%]	20.08	20.40	20.79	21.18	21.57	23.81
Volume of the dispersed phase *	[mL]	3.83	3.82	3.83	3.85	3.90	3.95
Hydrodynamic mean diameter **	[nm]	88 ± 8	92 ± 10	94 ± 15	97 ± 13	91 ± 7	75 ± 14
Average volume per droplet	[mL]	$3.57 \cdot 10^{-16}$	$4.08 \cdot 10^{-16}$	$4.35 \cdot 10^{-16}$	$4.78 \cdot 10^{-16}$	$3.95 \cdot 10^{-16}$	$2.21 \cdot 10^{-16}$
Droplets per batch	[-]	$1.07 \cdot 10^{16}$	$9.36 \cdot 10^{15}$	$8.81 \cdot 10^{15}$	$8.06 \cdot 10^{15}$	$9.88 \cdot 10^{15}$	$1.79 \cdot 10^{16}$
Mass per microgel	[g]	$7.48 \cdot 10^{-17}$	$8.76 \cdot 10^{-17}$	$9.54 \cdot 10^{-17}$	$1.07 \cdot 10^{-16}$	$8.90 \cdot 10^{-17}$	$5.59 \cdot 10^{-17}$
Microgels per mg	[mg^{-1}]	$1.34 \cdot 10^{13}$	$1.14 \cdot 10^{13}$	$1.05 \cdot 10^{13}$	$9.37 \cdot 10^{12}$	$1.12 \cdot 10^{13}$	$1.79 \cdot 10^{13}$
Molecular weight	[g mol^{-1}]	$4.55 \cdot 10^{7}$	$5.33 \cdot 10^{7}$	$5.80 \cdot 10^{7}$	$6.49 \cdot 10^{7}$	$5.41 \cdot 10^{7}$	$3.39 \cdot 10^{7}$

Tab. SI-9. Relevant parameter for the theoretical estimation of the microgels molar mass (II); varied polymeric solid content and constant crosslinker content (4.76 % (w/w)); *real volume of the disperse phase according to ESI-6; ** hydrodynamic man diameter measured as number weighted average by means of dynamic light scattering

Polymeric solid content	(w/w) [%]	2.56	10.14	20.79	30.02	40.11	50.04
Crosslinker content	(w/w) [%]	4.76	4.71	4.76	4.73	4.71	4.74
Volume of the dispersed phase *	[mL]	3.28	3.40	3.82	4.32	5.10	6.00
Hydrodynamic mean diameter **	[nm]	104 ± 6	80 ± 8	94 ± 15	109 ± 10	123 ± 15	180 ± 22
Average volume per droplet	[mL]	$5.59 \cdot 10^{-16}$	$2.68 \cdot 10^{-16}$	$4.35 \cdot 10^{-16}$	$6.60 \cdot 10^{-16}$	$9.98 \cdot 10^{-16}$	$3.05 \cdot 10^{-15}$
Droplets per batch	[-]	$5.57 \cdot 10^{15}$	$1.27 \cdot 10^{16}$	$8.81 \cdot 10^{15}$	$6.54 \cdot 10^{15}$	$5.11 \cdot 10^{15}$	$1.96 \cdot 10^{15}$
Mass per microgel	[g]	$2.15 \cdot 10^{-17}$	$2.85 \cdot 10^{-17}$	$9.54 \cdot 10^{-17}$	$2.10 \cdot 10^{-16}$	$4.19 \cdot 10^{-16}$	$1.63 \cdot 10^{-15}$
Microgels per mg	[mg^{-1}]	$4.65 \cdot 10^{13}$	$3.51 \cdot 10^{13}$	$1.05 \cdot 10^{13}$	$4.77 \cdot 10^{12}$	$2.38 \cdot 10^{12}$	$6.13 \cdot 10^{11}$
Molecular weight	[g mol^{-1}]	$1.38 \cdot 10^{7}$	$1.75 \cdot 10^{7}$	$5.80 \cdot 10^{7}$	$1.27 \cdot 10^{8}$	$2.54 \cdot 10^{8}$	$9.85 \cdot 10^{8}$

ESI-10: Static light scattering data, Zimm plots and molar mass

Tab. SI-10. Experimental refractive index increments for poly(acrylamide-co-sodium acrylate) microgels in water with varied polymeric solid content, constant cross linker content (4,76 % (w/w)) and constant sodium acrylate content (9,52 % (w/w)).

polymeric solid content (w/w) [%]	d*n*/d*c*
2.56	0.14
10.14	0.20
20.79	0.36
30.02	0.20
40.11	0.18
50.04	0.18

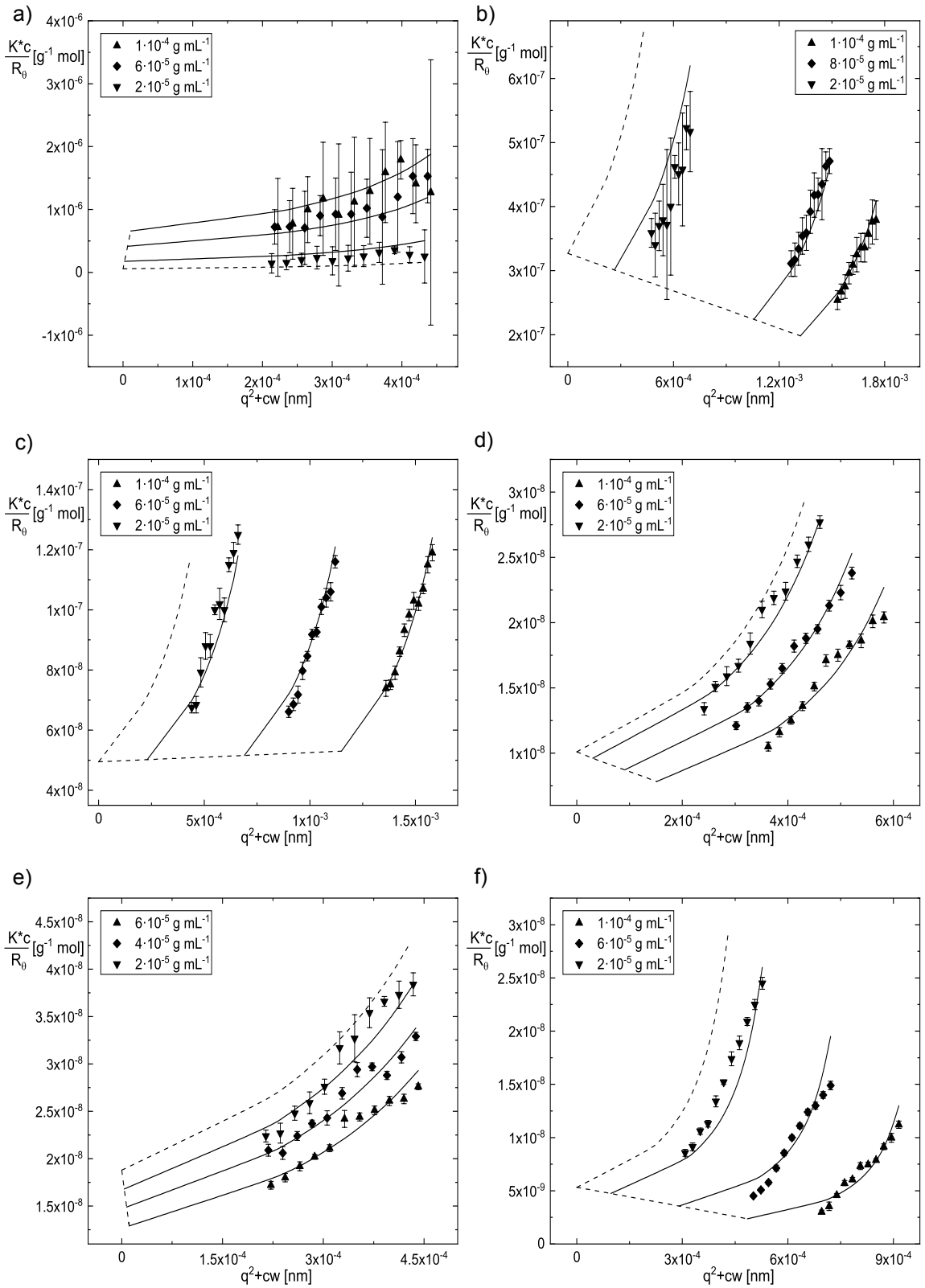

Fig. SI-10: Zimm plots based on light scattering data for poly(acrylamide-co-sodium acrylate) microgels with varied polymeric solid content, constant crosslinker content (4.76% (w/w)) and constant content of sodium acrylate (9.52% (w/w)) in water; polymeric solid content: (a) 2.56% (w/w), (b) 10.14% (w/w), (c) 20.79% (w/w), (d) 30.02% (w/w), (e) 40.11% (w/w), (f) 50.04% (w/w).

Tab. SI-11: Summary of static light scattering data for poly(acrylamide-co-sodium acrylate) microgels with varied polymeric solid content, constant crosslinker content (4.76 % (w/w)) and constant content of sodium acrylate (9.52% (w/w)) in water, including experimental M_{exp} and theoretical molar mass M_{theo}, hydrodynamic mean radius R_h, radius of gyration R_g and R_g/ R_h ratio.

Polymeric solid content (w/w) [%]	$M_{theo.}$ [a)] [g mol^{-1}]	$M_{exp.}$ [b)] [g mol^{-1}]	R_h [c)] [nm]	R_g [d)] [nm]	R_g/R_h [-]
2.56	$1.38 \cdot 10^7$	$1.79 \cdot 10^7$	94.5	67.4	0.713
10.14	$1.75 \cdot 10^7$	$3.06 \cdot 10^6$	76.5	59.9	0.783
20.79	$5.80 \cdot 10^7$	$2.02 \cdot 10^7$	83.5	63.2	0.757
30.02	$1.27 \cdot 10^8$	$9.94 \cdot 10^7$	89.0	67.6	0.760
40.11	$2.54 \cdot 10^8$	$5.32 \cdot 10^7$	75.5	62.6	0.828
50.04	$9.85 \cdot 10^8$	$1.88 \cdot 10^8$	100	75.5	0.755

a) The estimation of M_{theo} has been done as described in ESI-9; b) M_{theo} has been measured by static light scattering c) R_h has been measured as number weighted average by means of dynamic light scattering; d) R_g has been measured by static light scattering.

ESI-11: Deformability of microgels at low transmembrane pressures.

Differences between the various particle types, *e.g.* size, shape, particle size distribution, might significantly affect the cake structure and thus influence the absolute values of the hydraulic cake resistances. This, at least to some extent, reduces the value of information, accessible by direct comparison of different particle types by filter cake compressibility studies. To overcome this drawback, the gained data can be normalized to the hydraulic resistance, observed at the transmembrane pressure initially used to form the filter cake. However, this procedure is based on the idealized assumption that the particles are incompressible at this stage, still owning the full or at least about the same potential for deformation compared to that at higher pressure gradients.

It was found in this study, that the microgels already experienced a significantly deformed state when filter cakes have been created at 0.1 bar transmembrane pressure, analogously to the study by Helling et al. [12] Fig. SI-11 revels that the increase of the normalized specific cake resistance with transmembrane pressure for soft microgels, *i.e.* low crosslinker content and low polymeric solid content, is less pronounced compared to medium soft or more rigid microgels. This indicates that these materials are already in a highly deformed mode at an initial pressure stage in the experiment, thus having less susceptibility for further deformation. Medium soft microgels showed less initial deformation, consequently owning the potential for more pronounced deformation with increasing transmembrane pressure. More rigid microgels, *i.e.* those with high crosslinker and polymeric solid content, combining less initial deformation with lower potential for further deformation, resulting in lower slope of the rise in normalized specific cake resistance with transmembrane pressure. Overall, these tendencies are more pronounced with variation of the polymeric solid content (*cf.* ESI Fig. SI-11).

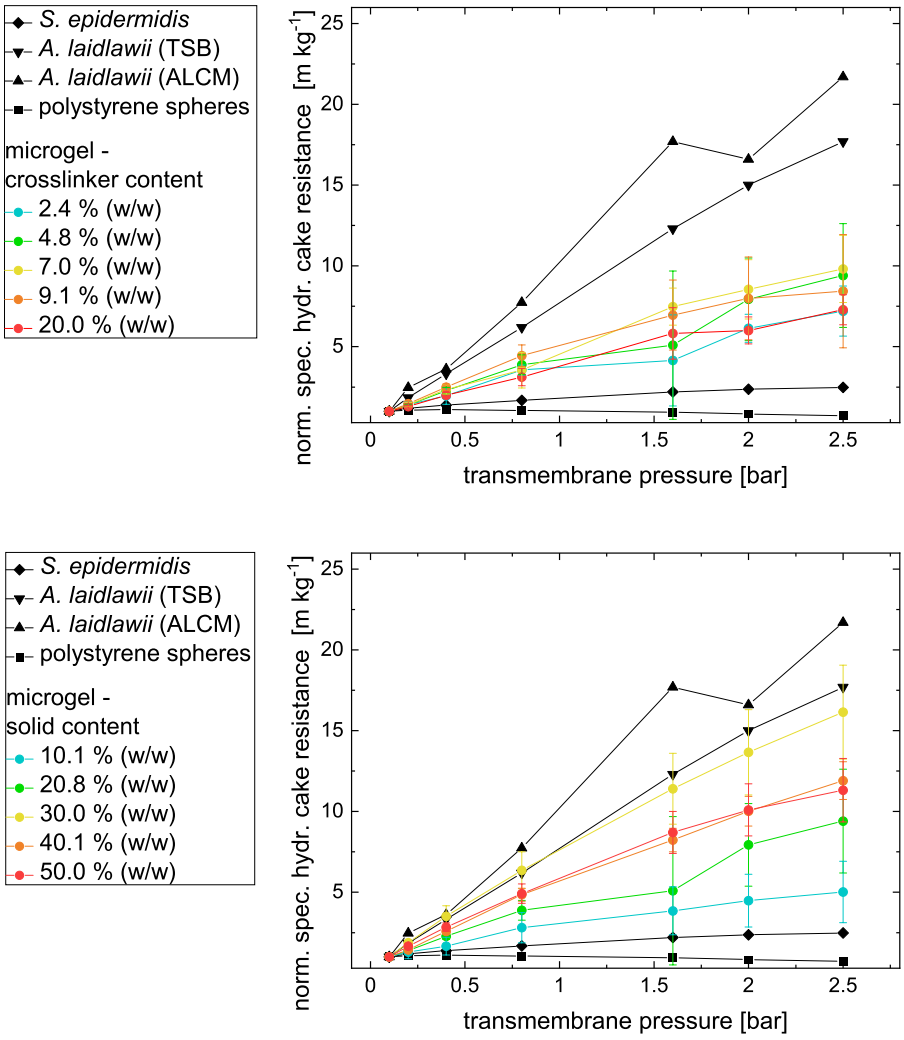

Fig. SI-11: Normalized specific hydraulic cake resistance of filter cakes consisting of microgels and relevant benchmark materials as function of applied transmembrane pressure at 20 °C media temperature. Microgels with varied cross-linker content, constant solid content (20 – 22% (w/w)) and constant content of AANa (9.52% (w/w)) (ID 2 – 6, cf. Table 2) (a) and microgels with varied solid content, constant cross-linker content (4.76% (w/w)) and constant content of sodium acrylate (9.52% (w/w)) (ID 8 – 11, cf. Table 2) (b) have been tested. Initially, filter cake formation has been conducted at 100 mbar. Normalization has been performed against specific hydraulic cake resistance of filter cakes at 100 mbar. Benchmark data from analogue experiments has been collected and published by Helling et al. [12] Here, *A. laidlawii* has been cultivated in a serum-free trypticase soy broth (**TSB**) [12, 13] or in a commercial *A. laidlawii* optimized cultivation media (ALCM) from Mycoplasma Experience (Bletchingley, UK) (**Mexp**). [12, 13] The symbols represent the mean and error bars the standard deviation of three individual measurements.

Additional measurements have been conducted, using 3 mbar transmembrane pressure for the initial filter cake formation (*cf.* ESI *Fig.* SI-12). Results support the hypothesis that the microgels are already significantly deformed at 0.1 bar transmembrane pressure. Again, no plateau has been observed at very low transmembrane pressures, indicating that, even at

3 mbar, the microgels are in a partially deformed state. Hypothetically, these findings can be explained by an adsorption of microgels on the membrane surface and their intrinsic tendency to spread on this solid/liquid interface. [14, 15] Due to adhesive forces, the microgels tend to deform under horizontal expansion and vertical compression, relative to the surface. This process is limited by the elastic restoring forces of the polymeric network, counteracting the adhesive forces and the provoked deformation. [16, 17] Consequently, microgels with a higher density of crosslinking points, *i.e*. higher crosslinker content or polymeric solid content, showed lower tendency to spread and deform on an interphase. [14, 18-20] This first layer of microgels, which is in direct contact to the membrane surface, might be deformed at infinitesimal transmembrane pressures, significantly affecting the hydraulic resistance of the filter cake. This hypothesis would explain the very large differences in initial specific cake resistance at 3 mbar, and their dependency on the crosslinker content as well as on the polymeric solid content (*cf.* ESI *Fig.* SI-12).

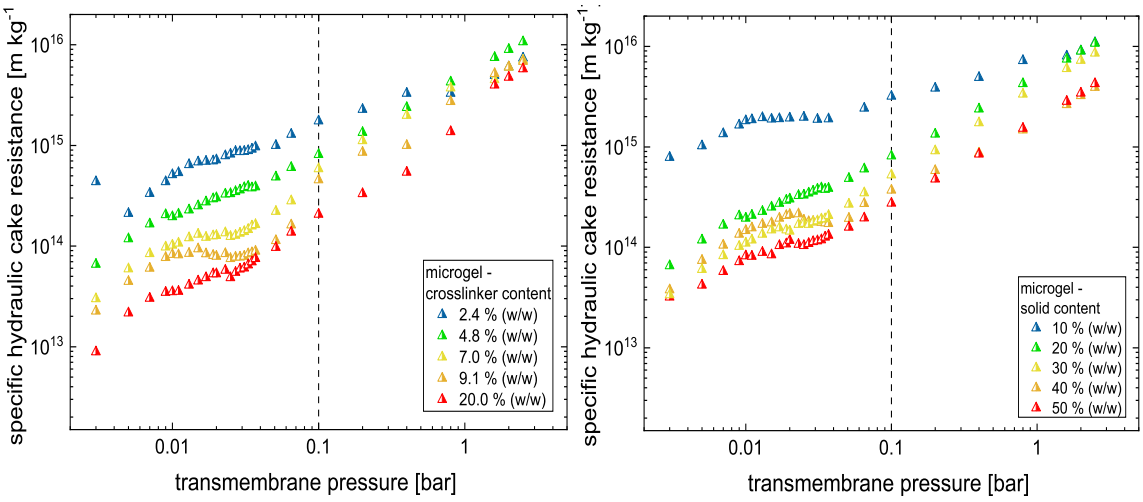

Fig. SI-12: Specific hydraulic cake resistance of filter cakes consisting of microgels as function of applied transmembrane pressure at 20 °C media temperature. Microgels with varied cross-linker content, constant solid content (20 – 22% (w/w)) and constant content of AANa (9.52% (w/w)) (ID 2 – 6, cf. Table 2) (a) and microgels with varied solid content, constant cross-linker content (4.76% (w/w)) and constant content of sodium acrylate (9.52% (w/w)) (ID 8 – 11, cf. Table 2) (b) have been tested. Initially, filter cake formation has been conducted at 3 mbar.

ESI-12: Additional Information for comparison of synthetic microgels with other particles

Tab. SI-12. Material properties of mycoplasma, microgels and selected benchmarks.

Particle/organism	Average hydrodynamic diameter	Structure	Zeta potential
A. laidlawii in TSB medium [a)]	840 ± 330 nm † [13, 21]	no rigid cell wall	-10 ± 1 mV [13, 21]
A. laidlawii in MKF medium [b)]	540 ± 230 nm † [13, 21]	no rigid cell wall	-23 ± 1 mV [13, 21]
A. laidlawii in Mexp medium [c)]	650 ± 260 nm † [13, 21]	no rigid cell wall	-2 ± 0.3 mV [13, 21]
S. epidermidis	1170 ± 220 nm † [13, 21]	rigid cell wall	-26 ± 1 mV * [13, 21]
Polystyrene spheres	792 ± 23 nm	hard particle	-52 ± 1 mV §
Soft / super soft microgels	180 ± 25 nm ‡	Hydrogel	-25 ± 10 mV #

[a)] Serum-free trypticase soy broth (TSB); [b)] serum containing cultivation medium according to Folmsbee (MKF); [13, 22] [c)] Commercial *A. laidlawii* optimated cultivation media (ALCM) from Mycoplasma Exerpience (Bletchingley, UK); [13] † Intensity weighted average hydrodynamic diameter (DLS-data); ‡ Number weighted average hydrodynamic diameter (DLS-data); ※ vendor datasheet; * in 20 mM sodium phosphate buffer; § in aqueous 0.26% (w/w) sodium dodecylsulfate (SDS) solution; # in aqueous 1 mM NaCl solution at pH 7.

ESI References

[1] I. Capek, *Adv. Colloid Interface Sci.* **2010**, *156*, 35-61

[2] G. Vitola, D. Büning, J. Schumacher, R. Mazzei, L. Giorno, M. Ulbricht, *Macromol. Biosci*. **2017**, *17*, 1600381.

[3] H. Durchschlag, P. Zipper, *Progr. Colloid Polym. Sci.* **1994**, *94*, 20-39.

[4] F. J. Millero, *Chem. Rev.* **1971**, *71*, 147-176.

[5] J. H. van't Hoff, *Z. Phys. Chem.* **1887**, *1*, 481-493.

[6] J. H. van't Hoff, „*Die Gesetze des chemischen Gleichgewichtes für den verdünnten gasförmigen oder gelösten Zustand*", Leipzig, Engelmann, **1900**.

[7] H. N. Morse, J. C. W. Frazer, F. M. Rogers, *Am. Chem. J.* **1907**, *38*, 175-226.

[8] K. Landfester, *Top. Curr. Chem.* **2003**, *227*, 75–123.

[9] M. A. Willert, *Prinzipien und Anwendungsmöglichkeiten nichtwäßriger und inverser Miniemulsionen*, Dissertation, University of Potsdam, Golm, **2001**.

[10] G. N. Lewis, *J. Am. Chem. Soc.* **1908**, *30*, 668-683.

[11] K. Landfester, *Annu. Rev. Mater. Res.* **2006**, *36*, 231–79

[12] A. Helling, V. Fischer, K. Eisfeld, K. Schmid, M. Polakovic, V. Thom, *Colloids Surf. B* **2020**, *185*, 110626.

[13] A. Helling, H. König, F. Seiler, R. Berkholz, V. Thom, M. Polakovic , *PDA J. Pharm. Sci. Technol.* **2018**, *72*, 264-277.

[14] G. Agrawal, R. Agrawal, *Polymers* **2018**, *10*, 418.

[15] F. A. Plamper, W. Richtering, *Acc. Chem. Res.* **2017**, *50*,131-140.

[16] J.-M. Y. Carillo, E. Raphael, A. V. Dobrynin, *Langmuir* **2010**, *26*, 12973-12979.

[17] T. Salez, M. Benzaquen, E. Raphael, *Soft Matter* **2013**, *9*, 10699.

[18] A. Burmistrova, M. Richter, C. Uzum, R. v. Klitzing, *Colloid Polym. Sci.* **2011**, *289*, 613-624.

[19] F. Schneider, A. Balaceanu, A. Feoktystov, V. Pipich, Y. Wu, J. Allgaier, W. Pyckhout-Hintzen, A. Pich, G. J. Schneider, *Langmuir* **2014**, *30*, 15317−15326.

[20] A. Mourran, Y. Wu, R. A. Gumerov, A. A. Rudov, I. I. Potemkin, A. Pich, M. Möller, *Langmuir* **2016**, *32*, 723-730.

[21] A. Helling, A. Kubicka, I. A. T. Schaap, M. Polakovic, B. Hansmann, H. Thiess, J. Strube, V. Thom, *J. Membr. Sci.* **2017**, *522*, 292-302.

[22] M. Folmsbee, K. R. Lentine, C. Wright, G. Haake, L. Mcburnie, D. Ashtekar, B. Beck, N. Hutchison, L. Okhio-Seaman, B. Potts, V, Pawar, H. Windsor, *PDA J. Pharm. Sci. Technol.* **2014**, *68*, 281-296.